Proceedings of the
15th International SPHERIC Workshop

June 8-11, 2021

Virtual Workshop

Edited by Dr. Angelo Tafuni

NEW JERSEY INSTITUTE OF TECHNOLOGY
Founded 1881

100 years
NEWARK COLLEGE OF ENGINEERING
NEW JERSEY INSTITUTE OF TECHNOLOGY

spheric
ERCOFTAC

ERCOFTAC

SPHERIC 2021

Proceedings of the 15th SPHERIC International Workshop

Virtual Workshop, 8-11 June 2021

Edited by

Angelo Tafuni

Published by New Jersey Institute of Technology

ISBN 978-0-578-91934-8

Acknowledgements

The 15th SPHERIC International Workshop is generously supported by the Newark College of Engineering of the New Jersey Institute of Technology and ERCOFTAC.

To my New Jersey Institute of Technology colleagues in the School of Applied Engineering and Technology, NCE Dean's Office, Office of the Provost, Office of Research, Strategic Events, Media Technology Support Services and many more: sincere thanks for your guidance and logistical assistance. This Workshop would not be possible without the support of the University's resources and community.

Foreword

Dear Delegate,

It is with great pleasure that I welcome you to the 15th SPHERIC International Workshop, the annual event dedicated to Smoothed Particle Hydrodynamics (SPH) and its advances. This year marks an important step as we reach the fifteenth edition of the workshop since the event's inception in 2006 and the first edition ever to run fully online. Regretfully, the COVID-19 pandemic has not made it possible to meet in the US in 2020 for what would have been the first SPHERIC Workshop taking place in America. However, as the World is starting to heal from this unfortunate pandemic, we all look forward to this year's fully online edition of the Workshop.

SPH was developed in the late 1970s to study astrophysics phenomena, but the last three decades have seen a remarkable diffusion of this particle method in several other fluid dynamics fields, such as flooding and tsunami inundation, wave breaking and wave-structure interaction, fluid-structure interaction, mixing processes, and jet impact. As the theoretical basis for SPH becomes increasingly secure, the range of applications rapidly expands also to thermally dominated processes, such as weld pools and power transfer systems (automotive and energy devices), where SPH simulations go beyond the state-of-the-art for CFD. The method has become ideal for inspiring early career researchers to make fundamental contributions to fluid mechanics.

A strong catalyzer behind the growth and success of SPH is the SPH rEsearch and engineeRing International Community (SPHERIC), founded in 2005 and at the center of many SPH initiatives, including SPHERIC Workshops, SPH Global seminars, student awards, newsletters, and much more. It has been an honor and a privilege to have joined the organization of such events by hosting this year's SPHERIC Workshop.

I look forward to welcoming you to the 15th SPHERIC International Workshop and to learning about your research. Thank you for being a part of this community.

Angelo Tafuni
New Jersey Institute of Technology
Chair, Local Organizing Committee,
15th SPHERIC International Workshop

Scientific Committee

Dr. Alex Crespo (Universidade de Vigo, Ourense, Spain)
Dr. Matthieu De Leffe (NEXTFLOW Software, France)
Dr. Xiangyu Hu (Technical University of Munich, Germany)
Dr. Abbas Khayyer (Kyoto University, Japan)
Dr. David Le Touzé (Ecole Centrale de Nantes, France)
Dr. Salvatore Marrone (CNR-INM, Italy)
Dr. Nathan Quinlan (National University of Ireland, Galway, Ireland)
Dr. Benedict Rogers (University of Manchester, UK)
Dr. Pierre Sabrowski (Dive Solutions, Germany)
Dr. Stefano Sibilla (Università di Pavia, Italy)
Dr. Antonio Souto Iglesias (UPM, Spain)
Dr. Angelo Tafuni (New Jersey Institute of Technology, US)
Dr. Renato Vacondio (Università di Parma, Italy)
Dr. Rade Vignjevic (Brunel University London, UK)
Dr. Giuseppe Bilotta (Istituto Nazionale di Geofisica e Vulcanologia, Italy)
Dr. Ha Bui (Monash University, Australia)
Dr. Andrea Colagrossi (CNR-INM, Italy)
Dr. Raj Das (RMIT University, Australia)
Dr. Walter Dehnen (University of Leicester, UK)
Dr. Peter Eberhard (University of Stuttgart, Germany)
Dr. Marco Ellero (Basque Center for Applied Mathematics, Spain)
Dr. Rouhollah Fatehi (Persian Gulf University, Iran)
Dr. Moncho Gómez-Gesteira (Universidade de Vigo, Spain)
Dr. Steven Lind (University of Manchester, UK)
Dr. Moubin Liu (Peking University, China)
Dr. Pablo Lorén-Aguilar (University of Exeter, UK)
Dr. Daniel Price (Monash University, Australia)
Dr. Pengnan Sun (Sun Yat-sen University, China)
Dr. Alexandre Tartakovsky (University of Illinois Urbana-Champaign, US)

Organizing Committee (New Jersey Institute of Technology)

Dr. Angelo Tafuni
Ms. Kimberly Dripchak
Dr. Moshe Kam
Dr. Ashish Borgaonkar
Dr. Samuel Lieber
Mr. Francesco Ricci

Table of Contents

5 – Convergence, Consistency and Stability 2

6 – Adaptivity and Variable Resolution

7 – Viscosity and Turbulence

8 – Complex Physics

9 – Coupling with Other Methods

10 – Free Surface Flows and Hydraulics

11 – Convergence, Consistency and Stability 3

12 – Free Surface and Moving Boundaries

Da Vinci's observation of turbulence: a study that aims to reproduce with the δ-LES-SPH method the physics behind one of his drawings

A. Colagrossi, S.Marrone
CRN-INM
Institute of Marine Engineering
Rome, Italy
andrea.colagrossi@cnr.it

P. Colagrossi
Punkt.ink
Rome, Italy
p.colagrossi@punkt.ink

D. Le Touzé
LHEEA Lab. (ECN and CNRS)
Ecole Centrale Nantes
Nantes, France
David.LeTouze@ec-nantes.fr

***Abstract*—This research activity was started in 2019 for the 500th anniversary of Leonardo da Vinci's death. Our Italian-French research group focused its attention on a famous drawing of da Vinci where a water jet impacts on a pool (RCIN 912660 The Windsor Collection). This particular drawing has been often used by many fluid dynamicists as a first important document concerning turbulent flows. It is worth noting that the word "turbulence", one of the most important phenomena in fluid dynamics, was used for the first time by da Vinci, in the "Atlantic codex". After a detailed study of different historical documents, we tried to reproduce with the δ-LES-SPH model at best the flow drawn in the sheet RCIN 912660, in order to better analyze the different descriptions that Leonardo reported beside his drawing.**

I. Introduction

Water flows obsessed Leonardo throughout his life (1452-1519). In the years between 1508 and 1511 he studied hydraulics in great detail with the unrealised intention of compiling a treatise on the subject. Leonardo made hundreds of observations on the movement of water and left astute analyses of complex motions in terms of linear and circular components. The superabundance of particular cases and the lack of mathematical tools (it was 300 years before Navier and Stokes) prevented him from ever realizing a set of generally applicable laws.

In 2019 there was the 500th anniversary of Leonardo da Vinci's death and for this event we planned to present a joint work at the scientific dissemination event "La fête de la Science 2019" in Nantes, France. This study started after a collaboration of fifteen years between our Italian-French research groups. Both groups are involved in the study of free-surface flows and develop numerical models for the investigation of such kinds of flows. The main idea was to reproduce one of Leonardo's drawings with in-house solvers developed by the two groups, to see if through the analysis of the simulations we would be able to recognize the descriptions written by Leonardo on his notes.

One of the inspirations of this work is also the fact that CNR-INM is based in Rome and ECN in Nantes which is an ideal prolongation of the the path between the cities of Vinci in Italy and Amboise in France which Leonardo travelled when he was invited by King Francis I of France. He settled in the Manor of Clos-Lucé in Amboise which was his residence in his last three years of life.

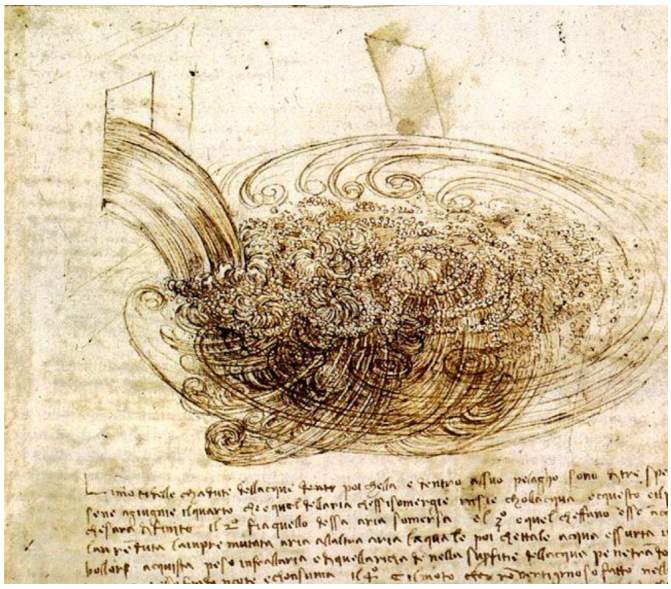

Fig. 1. Leonardo da Vinci's Studies of water (c.1510–12). The fall of a stream of water from a sluice into a pool. Bottom part of the sheet RCIN 912660 - The Windsor Collection.

We started our investigation from the word "turbulence". Indeed, this phenomenon of paramount importance in fluid dynamics was named for the first time by da Vinci. A famous drawing by Leonardo, reported in Fig. 1 and labeled as sheet RCIN 912660 of the Windsor collection, where a water jet impacts a water pool has been largely used by fluid dynamicists as an example of a turbulent flow, because this drawing is supposed to be one of the first illustration of what turbulence can be (see, *e.g.*, [8] [20]). Indeed, Leonardo represented the intrinsic three-dimensional nature of this turbulent flow with the idea that it consisted of a set of coexisting eddies ranging in scale from large to small. This concepts was formalized

mathematically 400 years later in 1941 by A.N. Kolmogorov and known as the "cascade model of turbulence" [11].

In this framework the present work is outlined trying to address the following questions:

1) What was actually represented by Leonardo (size, conditions, flow characteristics...)?
2) How can we reproduce it numerically?
3) Is it possible to simulate and visualize up to the details da Vinci drew?
4) Was Leonardo really describing underwater phenomena that he could not even see?

II. Methodology of investigation

In this section we describe the methodology of investigation we pursued. Firstly, we studied the story of Leonardo's hydraulic drawings, of his scientific environment at that time and the related analyses in the modern literature. As a second step we focused our attention on the RCIN 912660 drawing finding how specific it is among the body of all his hydraulic drawings. To perform this step we got into the story of RCIN 912660 in depth with the help of historians of art. After this investigation an analysis of the configuration represented in RCIN 912660 was achieved in terms of the geometrical settings (sizes of the sluice and pool, height of the water jet, depth of the pool, etc.) and the flow conditions (flow rate, incoming level of turbulence, air content in the jet, etc.) in order to reproduce it numerically. To improve this analysis we also paid attention to the sentences written under this drawing where Leonardo describes his understanding of the characteristics of the flow he drew. We have combined Leonardo's notes with an analysis of the flow characteristics according to our modern physics: intensity of turbulence, characteristics of the vortex scales, complex interaction between air and water, deformation of the free-surface and air bubbles entrapped inside the pool.

In order to plan the simulations we did several preliminary simulations changing different configurations and parameters. Once the final configuration had been selected, the use of cutting-edge supercomputer was needed to manage simulations with several tens of millions of particles. During the post-processing procedure we used advanced techniques in terms of visualization, graphic rendering, to be able to interpret the results of the large simulations. Finally, using our best results we performed a comparison of the numerical simulation to what was depicted and commented by Leonardo in his drawing.

III. The Windsor Collection, Leonardo da Vinci's Studies of water (c.1510–12)

The bottom part of the RCIN 912660 contains the drawing which is the subject of the present work (see Fig. 1): the fall of a stream of water from a gate into a pool in which multiple layered vortices are seen extending far below the surface, and where entrapment of air and the subsequent upward movement of air bubbles is also evident. From this drawing and the notes reported alongside, it is evident that Leonardo focused his attention on the air-water interactions, as he wrote:

"the beautiful movements which result from one element [air] penetrating another [water]".

The drawings exemplify Leonardo's ability to capture a momentary impression in his mind and fix it on paper. Then looking at the sentences Leonardo wrote below the drawing we found the details of the flow features identified by him. He recognized that the movements of air and water as it falls into the pool are of five kinds:

1) the air submerging with the water,
2) the motion of the submerged air which raises in the shape of large bubbles,
3) the upward movement produced by the water transported with the raising air bubbles when they ascend back to the water surface,
4) the downward movement produced by the water that continues its way towards the bottom which it strikes and consumes,
5) the eddy movements made on the pool surface by the water that comes back to the place of its fall this being the lowest place between the reflected and the impinging water.

A numerical simulation able to replicate those observations would allow to discuss in a modern way these kinds of phenomena. In particular it would be possible to evaluate the relevance of the turbulent structures developed by the shear layers generated by the falling water jet inside the water pool, with respect to the turbulence generated by the motion of the entrapped air which rises up toward the pool surface in the form of a bubble cloud. Another aspect which remains unclear from the examined drawing and on which a numerical simulation could shed some light, is how the water pool surface is affected by the above two sources of turbulence and how intense are the surface eddies and the gravity waves generated from it.

IV. Numerical simulation for reproducing the RCIN 912660 flow conditions

A. Multi-phase δ-LES-SPH model

A first attempt to reproduce the RCIN 912660 drawing was done by Monaghan & Kajtar using the Smoothed Particle Hydrodynamics (SPH) method [12]. That study was performed in a two-dimensional framework without taking into account the presence of the air. With this too restrictive simplified conditions the dynamics of the flow is quite different with respect to what described by Leonardo. On the other hand, that work showed the capabilities of this numerical method in simulating turbulent flows where an air-water interface is present, therefore inspiring the present study. Among the different variants of SPH developed during the last decades we select the δ-LES-SPH model described in [6] and recently further extended in [1]. In the present work the δ-LES-SPH model has been adapted to the multi-phase flow context following the work of Hammani et al. [10]. In the latter the pressure field is linked to the density field through the use of

a stiff equation of state:

$$p_i = f_\chi(\rho_i) = \frac{\rho_{0\chi} c_{0\chi}^2}{\gamma_\chi}\left[\left(\frac{\rho_i}{\rho_{0\chi}}\right)^{\gamma_\chi} - 1\right], \quad \forall\, i \in \chi \tag{1}$$

where γ_χ is the polytropic coefficient of phase χ and $c_{0\chi}$ is its speed of sound (χ being air or water in the present work). It is worth stressing that state equation (1) is adopted for both air and water phases, as the latter are treated as weakly-compressible media. Regarding the speeds of sound the procedure to select suitable values can be found in [10].

In the following text the δ-LES-SPH model is briefly recalled. For the sake of brevity only the most relevant information is reported, the interested reader is encouraged to find all the details in the cited articles. The governing equations are the Navier-Stokes equations which are discretized within the SPH context as follows:

$$\begin{cases} \dfrac{\mathrm{d}\rho_i}{\mathrm{d}t} = -\rho_i \displaystyle\sum_j (\boldsymbol{u}_{ji} + \delta\boldsymbol{u}_{ji}) \cdot \nabla_i W_{ij}\, V_j + \mathcal{D}_i^\rho + \\ \qquad\qquad + \displaystyle\sum_{j\in\chi} (\rho_j\, \delta\boldsymbol{u}_j + \rho_i\, \delta\boldsymbol{u}_i) \cdot \nabla_i W_{ij}\, V_j \\ \rho_i \dfrac{\mathrm{d}\boldsymbol{u}_i}{\mathrm{d}t} = - \displaystyle\sum_j F_{ij}^p \nabla_i W_{ij}\, V_j + \\ \qquad\qquad + \displaystyle\sum_{j\in\chi} (\rho_j\, \boldsymbol{u}_j \otimes \delta\boldsymbol{u}_j + \rho_i\, \boldsymbol{u}_i \otimes \delta\boldsymbol{u}_i) \cdot \nabla_i W_{ij}\, V_j + \\ \qquad\qquad + \boldsymbol{F}_i^v + \boldsymbol{F}_i^{st} + \rho_i \boldsymbol{g} \\ \dfrac{\mathrm{d}\boldsymbol{r}_i}{\mathrm{d}t} = \boldsymbol{u}_i + \delta\boldsymbol{u}_i, \;\; V_i = m_i / \rho_i, \;\; p_i = f_\chi(\rho_i), \;\forall i \in \chi \end{cases} \tag{2}$$

where the subscripts i and j refer to the generic i-th and j-th particles, $\boldsymbol{F}_i^v$ and $\boldsymbol{F}_i^{st}$ are the viscous and surface tension forces respectively acting on particle i while F_{ij}^p is the pressure force exchanged between the two particles. The vector field $\delta\boldsymbol{u}$ is the Particle Shifting velocity adopted to regularize the particles' spatial distribution during their motion. The notation $\boldsymbol{u}_{ji}$ indicates the difference $(\boldsymbol{u}_j - \boldsymbol{u}_i)$ and the same holds for $\delta\boldsymbol{u}_{ji}$ and $\boldsymbol{r}_{ji}$. χ denotes the phase of particle i; summations for $j \in \chi_i$ are thus computed only using particles belonging to the same phase.

The particle masses m_i are assumed to be constant during their motion. The particles are set initially on a Cartesian lattice with spacing Δr, and hence, the particle volumes V_i are evaluated initially as Δr^n with n the number of spatial dimensions of the problem, and the particle masses m_i are calculated through the initial density field (using the equation of state and the initial pressure field). During the time evolution, the volumes V_i change accordingly with particle densities ρ_i. The spatial gradients are approximated through convolution summation with a kernel function W_{ij}. As in [1] a C2-Wendland kernel is adopted in the present work.

The term $\mathcal{D}_i^\rho$ is the numerical diffusive term introduced by [3] to filter out the spurious high-frequency noise in the pressure field. Following [1] this term is rewritten within an LES framework as follows:

$$\begin{cases} \mathcal{D}_i^\rho := \displaystyle\sum_{j\in\chi} \delta_{ij}\, \boldsymbol{\psi}_{ji} \cdot \nabla_i W_{ij}\, V_j\,, \\ \boldsymbol{\psi}_{ji} := \left[(\rho_j - \rho_i) - \dfrac{1}{2}\left(\langle\nabla\rho\rangle_i^L + \langle\nabla\rho\rangle_j^L\right)\cdot \boldsymbol{r}_{ji}\right] \dfrac{\boldsymbol{r}_{ji}}{\|\boldsymbol{r}_{ji}\|^2} \\ \delta_{ij} := 2\, \dfrac{\nu_i^\delta\, \nu_j^\delta}{\nu_i^\delta + \nu_j^\delta}\,, \qquad \nu_i^\delta := (C_\delta\, l)^2\, \|\mathbb{D}_i\| \end{cases} \tag{3}$$

In the first equation since the summation is based on the χ phase the density diffusion is blocked across the air water interface. The constant C_δ is a dimensionless constant set equal to 6 while $l = 3\Delta r$ is the radius of the kernel support adopted in 3D simulations and represents the length scale of the filter adopted for the sub-grid model. The tensor $\mathbb{D}$ is the symmetric part of the velocity gradient and $\|\mathbb{D}\|$ is a rescaled Frobenius norm, namely $\|\mathbb{D}\| = \sqrt{2\mathbb{D} : \mathbb{D}}$. The superscript L in (3) indicates that the gradient is evaluated through the renormalized gradient equation, see [3].

The viscous forces $\boldsymbol{F}^v$ are expressed as:

$$\begin{cases} \boldsymbol{F}_i^v := 2(n+2) \displaystyle\sum_j (\mu_{ij} + \mu_{ij}^T)\, \pi_{ij}\, \nabla_i W_{ij}\, V_j\,, \\ \mu_{ij} := 2\, \dfrac{\mu_i\, \mu_j}{\mu_i + \mu_j}\,, \qquad \pi_{ij} := \dfrac{\boldsymbol{u}_{ij}\cdot\boldsymbol{r}_{ij}}{\|\boldsymbol{r}_{ji}\|^2}\,, \\ \mu_{ij}^T := 2\, \dfrac{\mu_i^T\, \mu_j^T}{\mu_i^T + \mu_j^T}\,, \qquad \mu_i^T := \rho_0\, (C_S\, l)^2\, \|\mathbb{D}_i\| \end{cases} \tag{4}$$

where n is the number of spatial dimensions and μ is the dynamic viscosity of the specific phase related to the particle i or j. This viscous term contains both the effect of the real viscosity μ and the one related to the local turbulent viscosity μ^T which is modelled through a simple Smagorinsky model where the constant C_S is set equal to 0.18 (see [16]).

Regarding the pressure force F_{ij}^p this corresponds to a switch from the "plus" formulation (namely, $F_{ij}^p = p_j + p_i$) to the "minus" form (that is, $F_{ij}^p = p_j - p_i$) when the pressure p_i is negative, namely:

$$F_{ij}^p = p_j + |p_i| \tag{5}$$

This switch allows to remove the so-called "tensile instability" which is a numerical instability of the SPH scheme. As remarked in Sun et al. [18] especially for high Reynolds number regimes the tensile instability can induce numerical cavitation in the cores of the eddies caused by the pressure drops inside these flow regions. Furthermore, even when such occurrence of numerical cavitation is prevented by the action of the shifting velocity $\delta\boldsymbol{u}$, it can alter the vorticity field adding numerical noise.

Similarly to what already underlined by [9], when using the models presented above to simulate multi-phase flows where surface tension effects are negligible, a non-physical inter-penetration of particles belonging to different phases may occur, leading to a numerical fragmentation of the fluid

interfaces. In order to prevent this, a small repulsive force has been introduced to mimic a surface tension force:

$$\boldsymbol{F}_i^{st} = \epsilon_\chi \sum_{j \in \overline{\chi}} \left(|p_i| + |p_j| \right) \nabla W_{ij} V_j \qquad (6)$$

where ϵ_χ is a parameter ranging between 0.01 and 0.1. The second summation applies to particles that do not belong to the fluid of the i-th particle. This set of particle is noted by $\overline{\chi}$. As shown in [5], eq. (6) models a cohesion force, *i.e.* a surface tension, as also explained in [13]. In Szewc et al. [19] it is shown in a heuristic way how the spurious interface fragmentation in multiphase SPH can be controlled by the coefficient ϵ_χ.

Finally, the Particle Shifting velocity $\delta\boldsymbol{u}$ is the one used in [17]. As documented in [17], the use of the Particle Shifting Technique (PST) leads to regular particle distributions and increases the accuracy and the robustness of the scheme. In turn, the inclusion of the PST causes the loss of the exact conservation of the angular momenta as commented in [17] and in [2].

B. Simulation set-up

As mentioned above the first problem in numerically reproducing the flow drawn by Leonardo Da Vinci in the sheet RCIN 912660 is the fact that we have no indications about the geometry and the flow conditions. Therefore, we started with performing some preliminary tests in order to set the simulation parameters in terms of:

- Determination of the problem geometry:
  - jet dimension and height above the pool,
  - pool size,
  - walls and outlet configuration,
  - inlet conditions.
- Identification of numerical parameters and CPU requirements: parameters linked to the SPH model presented in section IV-A, particle size, etc.
- Study of the relevance of air-entrainment and the effect of the percentage of air/water mixture.
- Detection and visualization of the vortex structures (Q-criterion, vorticity modulus, Finite Time Lyapunov Exponent).

On the base of the limits encountered in the study by [12], all the simulations of the present study, including this preliminary stage of the work, were performed in the three-dimensional framework.

C. Single-phase simulations

The simulations were performed using a numerical domain configuration in which the water is allowed to exit from three sides of the pool and the water jet is generated using an inlet over the pool. Fig. 2 reports a slice plot extracted from preliminary tests. In this simulation the particle resolution is $H_J/\Delta r = 60$ where H_J is the size of the considered-square jet at the inflow boundary. The inflow velocity U was set equal to 1.5 m/s, $H_J = 0.4$ m while the initial water height in the pool is $H_P = 2.7\,H_J$ m. It follows that the Froude number is $\mathrm{Fr} = U/\sqrt{g\,H_J} = 0.757$ while the Reynolds number was set equal to $\mathrm{Re} = \rho U H_J/\mu = 600,000$ by adopting the density and dynamic viscosity of the water. For this test the inflow conditions were prescribed by imposing a vertical velocity profile which mimics the boundary layer effects of a sluice gate. As a consequence the vorticity field inside the jet is not uniform and its free surface presents irregularities linked to the flow instability. The latter induces quicker inception of the instability of the shear layers developed in the pool. The resolution $H_J/\Delta r = 60$ is not enough to resolve all the scales of the inertial range.

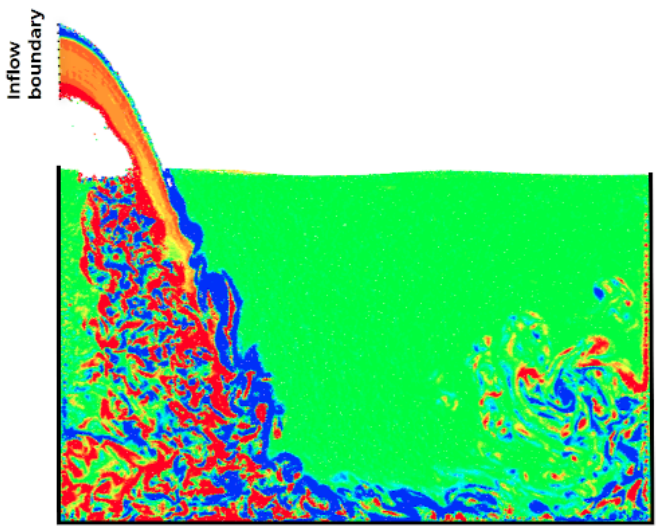

Fig. 2. SPH tests using a single-phase model (air phase is not included). Slice of the fluid domain in the $z-x$ mid plane at time 5.0 s. Colors are representative of the component of the vorticity field orthogonal to the slice (red clockwise, blue anticlockwise).

Left plot of Fig. 3 shows a 3D view of the water jet and of the water pool surface. Two slices of the flow domain are also reported with the particles colored with the y-vorticity. On the right plot the mid $z-x$ plane is colored with the modulus of the velocity. The maximum speed reached is about 4 m/s. From this contour plot the turbulent regime of the flow field can be clearly observed. The turbulent energy is mainly focused close to the shear layers while the rest of the domain remains almost at rest. This underlying structure of currents in sweeping whorls is very similar to what Leonardo tried to represent: indeed, it has been shown by art historians that Leonardo started his drawing with those vortex structures and then added the flow pattern linked to the air-water interaction [7].

In order to represent in a 3D view the vortical structures highlighted in Fig. 3 a post-processing of the SPH data is needed. For this procedure a subset of the particles is identified using the modulus of the vorticity field or using a Q-criterion. The vortical structures were better identified with this second choice so we used iso-contour of the Q field to proceed with

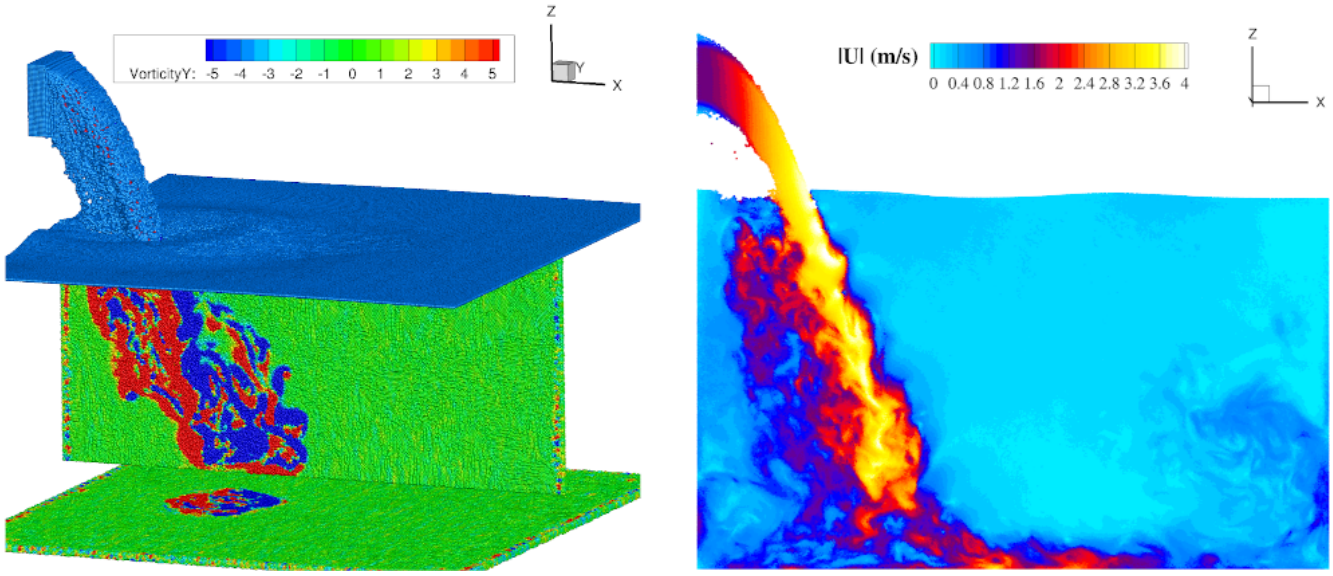

Fig. 3. SPH tests using a single-phase model (air phase is not included). Left: 3D view of the free surface with two slices of the domain where particles are colored with the y-vorticity component at time 1.5 s. Right: contour plot of the modulus of the velocity in the mid $z-x$ plane at time 5.0 s.

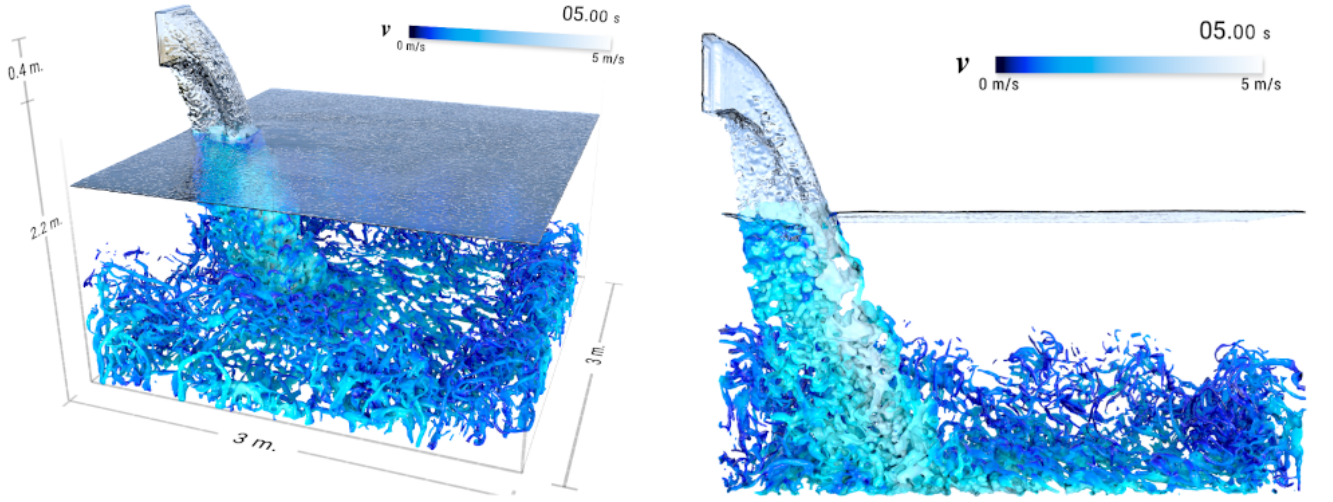

Fig. 4. SPH simulation using a single-phase model (air phase is not included). Rendering of the iso-surface $Q = 200\ s^{-2}$ and of the free surface. The iso-surface is colored with the intensity of the velocity field at time 5.0 s. Left: 3D view with the main lengths. Right: lateral view using half fluid domain.

the analysis. The latter is based on the equation:

$$Q = \frac{\mathbb{W}^2 - \mathbb{D}^2}{2} \tag{7}$$

where $\mathbb{W}$ is the anti-symmetric part of the velocity gradient tensor. For capturing the vorticity structures only the particles having a Q value greater than a certain positive threshold are selected.

Fig. 4 shows an iso-Q surface which is colored with the intensity of the velocity field to improve the rendering. In this figure the rendering of the free-surface is also presented. Remarkably, with this single-phase model the water pool surface remains almost flat and smooth and very far from what drawn by Leonardo. In the figure the main lengths of the problem are also reported.

The physical simulation time is 10.4 seconds and involved, in average, about 50 million particles for 37000 time iterations. The resolution is $H_J/\Delta r = 60$. The simulation ran for 102 hours on 360 cores on the "Liger" supercomputer at Ecole Centrale de Nantes which is equipped with 12-core Intel Xeon (Haswell) E5-2680v3 processors.

D. Air-water simulations

From the previous section it is clear that the modelling of the liquid phase alone is not enough to reproduce the flow drawn in the RCIN 912660 sheet. In order to get closer to Leonardo's drawing the air phase was added in the numerical model. As a first attempt, the air phase was firstly introduced

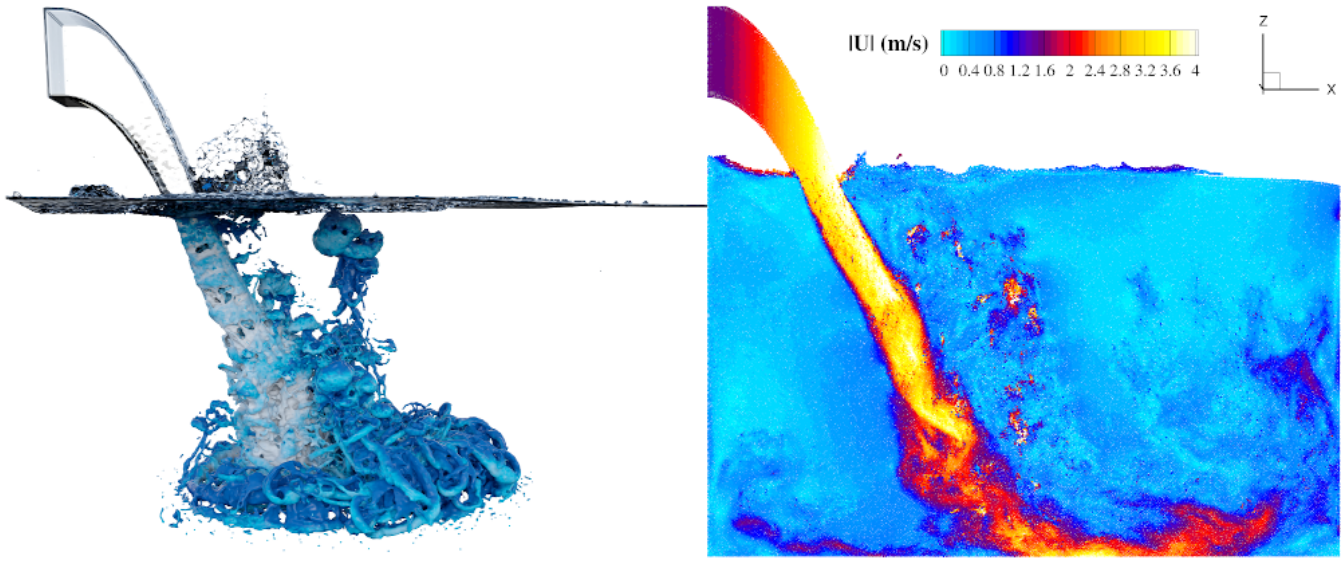

Fig. 5. SPH simulation using a air-water model. Left: lateral view of the rendering of the iso-surface $Q = 200\ s^{-2}$. This iso-surface is colored with the intensity of the velocity field at time 2.6 s. Right: mid $z - x$ plane colored with the modulus of the velocity at time 5.0 s.

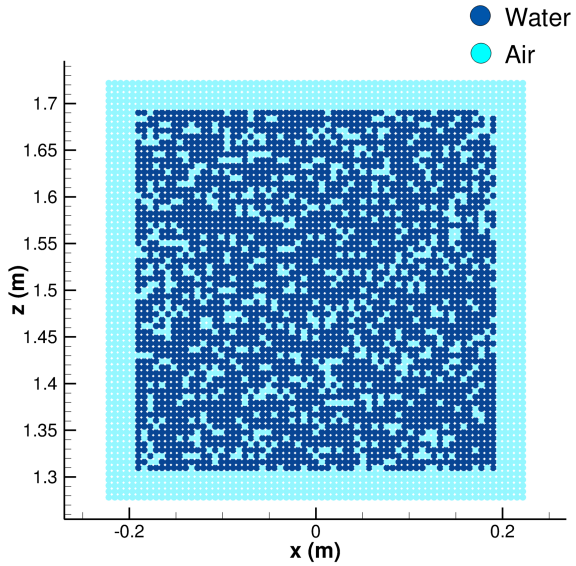

Fig. 6. SPH simulation using an air-water model: layout of the fluid particle phases generated in the inlet plane.

in the domain as dispersed in the water jet: following the work by Chanson et al. [4] a percentage of 20% of air inside the jet was used which corresponds to a characteristic value of a high air content in a supercritical channel flow. Hence, the air particles are positioned randomly in the inflow with a ratio 1:5 to the liquid particles.

However, as well known in the literature (see, *e.g.*, [14], [15]) the air entrapped in the shear layer during the jet penetration plays an important role too. This can be achieved by modelling the whole air domain with air particles. However, this would imply a large increase of CPU costs associated with the consequent increase of total particle number. In order to avoid this, in the inlet flow a frame of air particles was added surrounding the square section which originated the water jet. For the sake of clarity, in Fig. 6 the layout of the particles generated in the inlet plane is shown. In this way part of the air plunges in the water entrapped in the shear layer generated by the jet. This partial filling of the air domain is possible within the SPH model thanks to the equation of state (1) used. Indeed the air particles are surrounded by a free surface, *i.e.* a constant pressure acts on the modelled air domain surface and therefore the air particles are confined and do not wander from the jet. Because of the complexities related to the use of the air frame surrounding the water jet, in this configuration a uniform inlet velocity is enforced for both air and water particles. For the two-phase simulation the same resolution of the single-phase simulation phase has been adopted, $H_J/\Delta r = 60$. It involved about 50 million particles in average and ran on 720 cores for 107 hours to simulate 128,000 time steps, corresponding to a physical time of 8.4 seconds.

Left plot of Fig. 5 an iso-Q surface of the flow is depicted at $t = 2.6$ s. The air bubbles entrapped in the jet flow detach from the main current and rise towards the free surface. In their motion they generate vorticity associated to the boundary layer at the air-water interface which takes the form of a perturbation along the main jet current. It is also worth noting the complex toroidal vortex that is generated when the jet encounters the bottom of the tank. The annular vortex expands keeping an almost circular shape while further transverse vortices are formed running around the main vortex tube. In the right plot of Fig. 5 the contour plot of the velocity modulus for the air-water simulation is reported. Comparing this picture to its single-phase counterpart in Fig. 3 it can be noticed that in the two-phase simulation some turbulent structures detached in the fluid region in front of the jet.

Fig. 7. SPH simulation using an air-water model. Rendering of the air particles. 3D view at time instant 4.2 s.

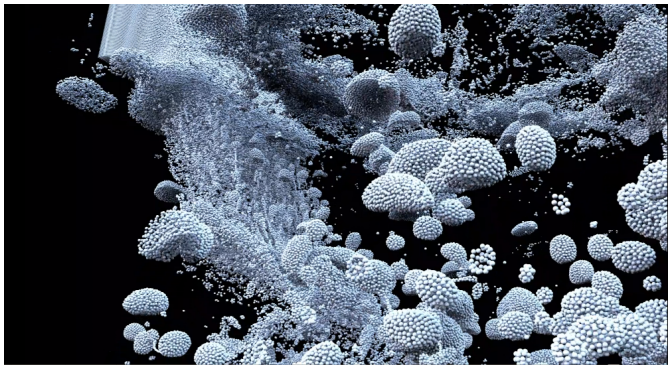

Fig. 8. SPH simulation using an air-water model. Rendering of the air particles. 3D view from bottom at time instant 8.4 s.

In Figs. 7 and 8 only the air particles are represented for two different time instants and from two different points of view: in the former the whole field is depicted at $t = 4.2$ s whereas in the latter a close view below the free surface in front of the jet is shown at $t = 8.4$ s. From these views, three different regions of the flow can be recognised:

1) the jet flow in which the air is dispersed and starts aggregating in the form of small bubbles;
2) the liquid region in front of the jet flow where larger bubbles are formed and rise towards the free surface interacting with each other;
3) the area on the free surface in front of the jet where the bubbles eventually burst creating "rosettes" similarly to what drawn by Leonardo.

In Fig. 9 a non-photorealistic rendering of the simulation using the same colors of Leonardo's drawing is presented. The figure highlights the air-water interaction on the pool surface. The bursting of the biggest air bubbles generate "rosette" shapes which is one of the main flow features stressed by Leonardo in the RCIN 912660 drawing. Fig. 10 depicts some particles trajectories from the inflow section up to their ascent to the pool surface. These curved trajectories is another flow feature stressed in the Leonardo drawing.

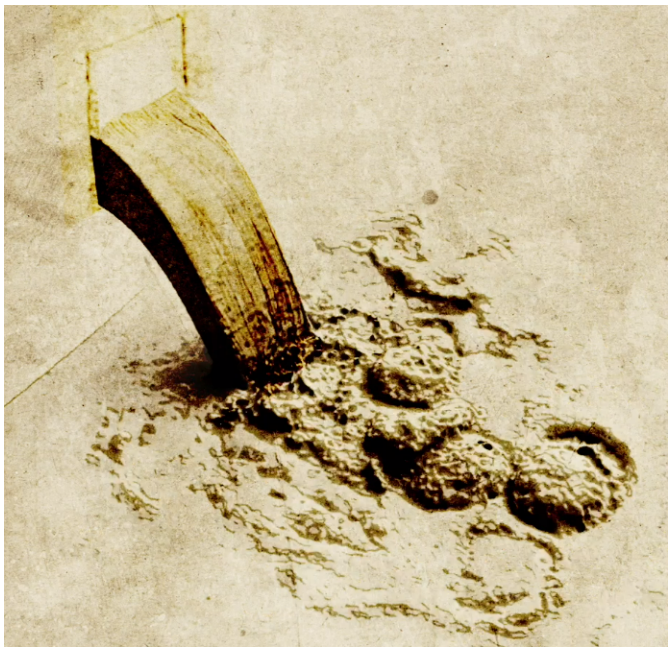

Fig. 9. SPH simulation using an air-water model. Non-photorealistic rendering, 3D view from the top at time instant 5.8 s.

When looking the post-processing of the present simulations and comparing them with the RCIN 912660 drawing what is still missing are the rounded curves/trajectories drawn by Leonardo on the pool surface. Our hypothesis is that these curves are mainly linked to the domain confinement and since in our simulation the flow exits from the lateral and the front sides of the domain, this recirculation is not present. Furthermore, this recirculating motion of the flow around the pool would have a characteristic time scale much longer then the few seconds computed in our simulation. This topic deserves further investigation and leaves the door open to further studies of the RCIN 912660 drawing.

V. Conclusion

500 years after the death of Leonardo Da Vinci in Amboise a French-Italian research team has tried to reproduce the physics behind one of his most famous and elaborate drawing of water studies. Leonardo Da Vinci was a fine observer of water flows. He was able to extract essential phenomena of complex air-water flows and accurately describe each flow feature independently from the others. The complexities of the flow features highlighted by Leonardo are linked to the vortical structures generated by a free surface flow where air entrainment plays a significant role. These conditions made the numerical simulation his drawing very challenging.

To tackle this problem a numerical method called Smoothed Particle Hydrodynamics (SPH) has been selected and its further extension to turbulent multi-phase flows, called δ-LES-SPH has been adopted by the team.

Initial difficulties arose from the lack of knowledge of

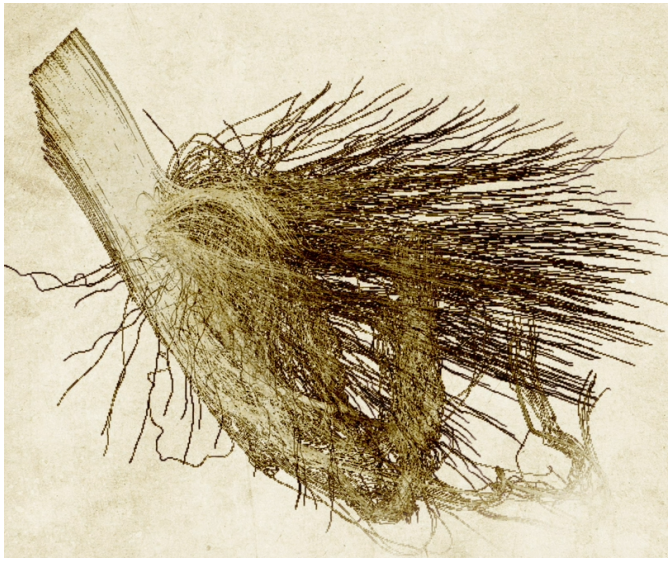

Fig. 10. SPH simulation using an air-water model. Trajectories of water particles from the inflow up to their ascent to the pool surface.

the flow conditions observed by Leonardo. Successive hypotheses have been made on the geometry and inflow and outflow. Three-dimensional numerical simulations have been performed on a supercomputer using tens of millions of fluid elements. A sophisticated graphical rendering was needed to visualize the large amount of data. First results showed that the role of the air entrained by the water jet is crucial in driving turbulent structures at the surface in front of the jet. In the end, in the final simulation run one can recognize very similar features to the ones in the drawing by Leonardo, but with much more details of course. And the analysis is still in progress.

Acknowledgments

The present research has been funded by Ecole Centrale de Nantes, providing technical and IT supports.

The SPH simulations performed under the present research have been obtained using the SPH-Flow solver, software developed within a collaborative consortium composed of Ecole Centrale Nantes, NextFlow Software company and CNR-INM.

The research activity has been developed within the Project Area Applied Mathematics of the Department of Engineering, ICT and Technology for Energy and Transport (DIITET) of the Italian National Research Council (CNR).

References

[1] M Antuono, S Marrone, A Di Mascio, and A Colagrossi. Smoothed particle hydrodynamics method from a large eddy simulation perspective. generalization to a quasi-lagrangian model. *Physics of Fluids*, 33(1):015102, 2021.

[2] M Antuono, PN Sun, S Marrone, and A Colagrossi. The δ-ALE-SPH model: An arbitrary lagrangian-eulerian framework for the δ-SPH model with particle shifting technique. *Computers & Fluids*, 216:104806, 2021.

[3] Matteo Antuono, Andrea Colagrossi, and Salvatore Marrone. Numerical diffusive terms in weakly-compressible sph schemes. *Computer Physics Communications*, 183(12):2570–2580, 2012.

[4] Hubert Chanson. Measuring air-water interface area in supercritical open channel flow. *Water Research*, 31(6):1414–1420, 1997.

[5] A. Colagrossi and M. Landrini. Numerical simulation of interfacial flows by smoothed particle hydrodynamics. *J. Comput. Phys.*, 191(2):448–475, November 2003.

[6] A Di Mascio, M Antuono, A Colagrossi, and S Marrone. Smoothed particle hydrodynamics method from a large eddy simulation perspective. *Physics of Fluids*, 29(3):035102, 2017.

[7] A. Donnithorne. *Leonardo Da Vinci: A Closer Look*. Royal Collection Trust, 2019.

[8] Robert Ecke. The turbulence problem: An experimentalist's perspective. *Los Alamos Science*, 29:124–141, 2005.

[9] Nicolas Grenier, Matteo Antuono, Andrea Colagrossi, David Le Touzé, and B Alessandrini. An hamiltonian interface sph formulation for multi-fluid and free surface flows. *Journal of Computational Physics*, 228(22):8380–8393, 2009.

[10] I Hammani, S Marrone, A Colagrossi, G Oger, and D Le Touzé. Detailed study on the extension of the δ-sph model to multi-phase flow. *Computer Methods in Applied Mechanics and Engineering*, 368:113189, 2020.

[11] Andrej Nikolaevich Kolmogorov. Equations of turbulent motion in an incompressible fluid. In *Dokl. Akad. Nauk SSSR*, volume 30, pages 299–303, 1941.

[12] Joseph John Monaghan and Jules Balazs Kajtar. Leonardo da vinci's turbulent tank in two dimensions. *European Journal of Mechanics-B/Fluids*, 44:1–9, 2014.

[13] S. Nugent and H.A. Posch. Liquid drops and surface tension with smoothed particle applied mechanics. *Physical Review E*, 62(4):4968, 2000.

[14] CD Ohl, HN Oguz, and Andrea Prosperetti. Mechanism of air entrainment by a disturbed liquid jet. *Physics of Fluids*, 12(7):1710–1714, 2000.

[15] A Prosperetti and HN Oguz. Air entrainment upon liquid impact. *Philosophical Transactions of the Royal Society of London. Series A: Mathematical, Physical and Engineering Sciences*, 355(1724):491–506, 1997.

[16] Joseph Smagorinsky. General circulation experiments with the primitive equations: I. the basic experiment. *Monthly weather review*, 91(3):99–164, 1963.

[17] PN Sun, A Colagrossi, S Marrone, M Antuono, and A-M Zhang. A consistent approach to particle shifting in the δ-plus-sph model. *Computer Methods in Applied Mechanics and Engineering*, 348:912–934, 2019.

[18] PN Sun, Andrea Colagrossi, Salvatore Marrone, Matteo Antuono, and AM Zhang. Multi-resolution delta-plus-sph with tensile instability control: Towards high reynolds number flows. *Computer Physics Communications*, 224:63–80, 2018.

[19] K. Szewc, J. Pozorski, and J.P. Minier. Spurious interface fragmentation in multiphase sph. *International Journal for Numerical Methods in Engineering*, 103(9):625–649, 2015.

[20] Hendrik Tennekes and John L Lumley. *A first course in turbulence*. MIT press, 2018.